Journal of the National Cancer Center 4 (2024) 346–353

Contents lists available at ScienceDirect

Journal of the National Cancer Center

journal homepage: www.elsevier.com/locate/jncc

Full Length Article

Construction and application of a three-dimensional vascular variation-based nephrometry scoring system for completely endophytic renal tumors

Aihetaimujiang Anwaier[1,2,3,†], Xiangxian Che[1,2,3,†], Lei Shi[4,†], Xi Tian[1,2,3], Shiqi Ye[1,2,3], Wenhao Xu[1,2,3,*], Yu Zhu[1,2,3,*], Hailiang Zhang[1,2,3,*], Dingwei Ye[1,2,3,*]

[1] Department of Urology, Fudan University Shanghai Cancer Center, Shanghai, China
[2] Shanghai Genitourinary Cancer Institute, Shanghai, China
[3] Department of Oncology, Fudan University Shanghai Medical College, Shanghai, China
[4] Department of Operating Room, Fudan University Shanghai Cancer Center, Shanghai, China

ARTICLE INFO

Keywords:
Completely endophytic renal tumors
Three-dimensional reconstructed images
Vascular variation
Nephrometry scoring system
Robot-assistant partial nephrectomy
Renal function

ABSTRACT

Background: Completely endophytic renal tumors (CERT) pose significant challenges due to their anatomical complexity and loss of visual clues about tumor location. A facile scoring model based on three-dimensional (3D) reconstructed images will assist in better assessing tumor location and vascular variations.

Methods: In this retrospective study, 80 patients diagnosed with CERT were included. Forty cases underwent preoperative assessment using 3D reconstructed imaging (3D-Cohort), while the remaining 40 cases were assessed using two-dimensional imaging (2D-Cohort). Vascular variations were evaluated by ascertaining the presence of renal arteries > 1, prehilar branching arteries, and arteries anterior to veins. The proposed scoring system, termed RAL, encompassed three critical components: (R)adius (maximal tumor diameter in cm), (A)rtery (occurrence of arterial variations), and (L)ocation relative to the polar line. Comparison of the RAL scoring system was made with established nephrometry scoring systems.

Results: A total of 48 (60%) patients exhibited at least one vascular variation. In the 2D-Cohort, patients with vascular variations experienced significantly prolonged operation time, increased bleeding volume, and extended warm ischemia time compared with those without vascular variations. Conversely, the presence of vascular variations did not significantly affect operative parameters in the 3D-Cohort. Furthermore, the 2D-Cohort demonstrated a notable decline in both short- and long-term estimated glomerular filtration rate (eGFR) changes compared with the 3D-Cohort, a trend consistent across patients with warm ischemia time ≥ 25 min and those with vascular variations. Notably, the 2D-Cohort exhibited a larger margin of normal renal tissue compared with the 3D-Cohort. Elevated RAL scores correlated with larger tumor size, prolonged operation time, extended warm ischemia time, and substantial postoperative eGFR decrease. The RAL scoring system displayed superior predictive capabilities in assessing postoperative eGFR changes compared with conventional nephrometry scoring systems.

Conclusions: Our proposed 3D vascular variation-based nephrometry scoring system offers heightened proficiency in preoperative assessment, precise prediction of surgical complexity, and more accurate evaluation of postoperative renal function in CERT patients.

1. Introduction

Renal cell carcinoma (RCC) is one of the most common solid tumors of the urinary system, accounting for 4.2% of all new cancer cases.[1] In the management of localized T1a RCC, partial nephrectomy (PN) has emerged as the gold standard, offering comparable oncologic control while preserving superior renal function compared with radical nephrectomy.[2,3] However, the treatment of completely endophytic renal tumors (CERT) presents unique challenges due to their complex anatomical characteristics and lack of visual cues for tumor localization. This complexity often results in prolonged operative time, increased intraoperative blood loss, extended ischemia time, compromised preservation of functional nephrons, and elevated postoperative creatinine levels.[4,5] In recent years, robot-assisted PN (RAPN) has gained widespread

* Corresponding authors.
E-mail addresses: xwhao0407@163.com (W. Xu), ronniezhu001@gmail.com (Y. Zhu), zhanghl918@alu.fudan.edu.cn (H. Zhang), dwyelie@163.com (D. Ye).
† These authors contributed equally for this study.

https://doi.org/10.1016/j.jncc.2024.06.001
Received 13 December 2023; Received in revised form 8 June 2024; Accepted 10 June 2024

acceptance due to its minimally invasive nature, precise surgical techniques, and early recovery benefits. Comparisons between laparoscopic PN (LPN) and RAPN consistently demonstrate the superior performance of RAPN in reducing ischemia time and lowering conversion rates.[6,7] Furthermore, the enhanced precision provided by robotic technology enables surgeons to overcome technical challenges associated with highly complex lesions, including completely endophytic renal tumors.[8] While RAPN has been proven to be an excellent approach for T1a RCC, preserving functional nephrons remains challenging when treating CERT.

Accurate tumor localization and assessment of tumor-related anatomy are crucial for effective planning of RAPN procedures. Nephrometry scoring systems, such as the R.E.N.A.L (radius [R], exophytic/endophytic properties [E], nearness of tumor to the collection system or sinus [N], anterior or posterior [A], location relative to polar lines [L]) nephrometry scoring system, PADUA (preoperative aspects and dimensions used for anatomy) classification system, and C-index (centrality index), provide detailed anatomical descriptions and quantify tumor complexity from various angles.[9-11] These scoring systems greatly improved the surgeons' ability to predict surgical complexity and peri- and postoperative complication rates and can assist in individualizing surgical protocol decision-making. However, most of the existing nephrometry scoring systems were based on traditional two-dimensional (2D) images, which has its intrinsic limitations and inaccuracy compared with three-dimensional (3D) reconstructed images.[12-14] Studies evaluating renal nephrometry scores using 3D reconstructed images have demonstrated higher inter-observer agreement compared with 2D imaging.[15,16] Additionally, a scoring system based on 3D reconstructed images has effectively stratified renal sinus tumors for surgical treatment, highlighting the advantages of 3D imaging in evaluating highly complex tumors like CERT.[17] Nevertheless, previous scoring systems have not incorporated vascular factors in assessing kidney and tumor blood supply.

Typically, each kidney receives arterial blood supply from a single renal artery branching from the abdominal aorta, with renal veins positioned anteriorly. However, approximately 25% to 50% of kidneys exhibit anatomical variations in the renal vascular system, particularly in the form of accessory renal arteries, prehilar branching, and arteries located anteriorly to veins.[18-20] These renal vascular variations pose challenges during surgical intervention and can lead to hemorrhage and compromised surgical field visualization. While previous nephrometry scoring systems have successfully assessed tumor complexity in CERT, they have failed to consider the impact of vascular factors on tumor resection.

Therefore, in this study, we aim to construct a quantifiable, intuitive, and easily applicable scoring model based on 3D reconstructed images that incorporates vascular variation factors. This scoring model will accurately describe the precise anatomical features and assess its predictive value in RAPN for CERT.

2. Materials and methods

2.1. Study design and patient populations

This retrospective cohort study included 80 patients with CERT who underwent RAPN at Fudan University Shanghai Cancer Center between December 2019 and December 2022. The patients were divided into two cohorts: a 3D cohort consisting of 40 patients assessed using preoperative 3D reconstructed imaging, and a 2D cohort consisting of 40 patients assessed using 2D imaging. The inclusion criteria were as follows: (I) patients with CERT (three points for the "E" element of the R.E.N.A.L. scoring system), (II) patients who received RAPN, (III) availability of preoperative enhanced radiographic images, (IV) normal contralateral kidney function, (V) no prior anti-tumor therapy, and (VI) Eastern Cooperative Oncology Group (ECOG) performance status 0–1.

2.2. Data collection and assessment

Clinical data, including age, gender, body mass index (BMI), history of hypertension and diabetes, tumor size, duration of surgery, bleeding volume, warm ischemia time, and creatinine levels, were collected from electronic medical records. The warm ischemia time of 25 minute (min) threshold was used as a cut-point according to previous studies.[21-23] The estimated glomerular filtration rate (eGFR) was calculated using the Modification Diet Renal Disease 2 equation.[24] All patients were performed preoperative enhanced computerized tomography (CT) or magnetic resonance imaging (MRI). For the 3D-Cohort, 3D images were reconstructed using enhanced CT or MRI. The number of renal arteries, prehilar branching artery, and artery anterior to the vein were evaluated using 2D and 3D images for the 2D- and 3D-Cohorts, respectively. Arterial variations were determined based on the presence of renal arteries > 1, the presence of a prehilar branching artery, and the presence of an artery anterior to the vein. The prehilar branching artery is defined as the primary branches of the renal artery being less than 1.5 centimeter (cm) from the root of the renal artery. Pathological sections were collected and independently assessed by two experienced genitourinary pathologists. Follow-up information was obtained during clinical visits or by telephone.

2.3. The RAL scoring system

To develop a more intuitive and quantifiable surgical complexity scoring system, we defined three critical components: (R)adius (maximal tumor diameter in cm), (A)rtery (occurrence of arterial variations), and (L)ocation relative to the polar line. Each component was scored on a 1 to 3-point scale, and the scores were added up to obtain the total RAL score. CERTs with RAL scores ranging from 3 to 4, 5 to 6, and 7 to 9 were classified as low, moderate, and high complexity lesions, respectively. Traditional scoring systems, including the R.E.N.A.L score, PADUA score, and CI score, were calculated based on 2D images. Receiver Operating Characteristics (ROC) curves were plotted and the area under the curve (AUC) was calculated to assess the predictive value of each scoring system using the "pROC" package of R language. The scoring systems were evaluated by two urologists and one radiologist, and the average score was used in the analysis.

2.4. Statistical analysis

Continuous variables were expressed as median (interquartile range [IQR]), and categorical variables were expressed as number (percentage). Paired data were analyzed using *t*-tests or Wilcoxon matched-pairs signed rank tests, while unpaired data were analyzed using unpaired *t*-tests or Mann-Whitney tests. The Kruskal-Wallis H test was used to compare continuous variables, and categorical variables were compared using the Pearson chi-square test. All statistical tests were two-sided, and *P*-values less than 0.05 were considered statistically significant. SPSS software and GraphPad Prism were used for data analysis and visualization, respectively.

3. Results

3.1. Patient characteristics

The study encompassed a cohort of 80 patients who underwent RAPN for CERT. All essential data were meticulously collected, with 40 patients evaluated preoperatively using 3D reconstructed images (3D-Cohort), while the remaining 40 patients were assessed using conventional 2D images (2D-Cohort). The overall characteristics of all patients are summarized in Table 1. The median age was 52 (IQR: 44.3–65.5) years, 52 patients were male (65%), 28 (35%) patients were female, and the median tumor size was 2.5 cm (IQR: 1.8–3.0). The median BMI

Table 1
Clinicopathological futures and vascular variation.

Variable	Total (n = 80)	3D Cohort (n = 40)	2D Cohort (n = 40)	P value
Age, median (IQR), years	52.0 (44.3, 65.5)	52.0 (45.3, 65.5)	53.0 (44.3, 65.5)	ns
Gender, No. (%)				ns
Male	52.0 (65.0)	24.0 (60.0)	28.0 (70.0)	
Female	28.0 (35.0)	16.0 (40.0)	12.0 (30.0)	
Tumor size, median (IQR), cm	2.5 (1.8, 3.0)	2.5 (1.8, 3.0)	2.3 (1.8, 3.0)	ns
Pathological type, No. (%)				ns
ccRCC	73.0 (91.3)	37.0 (92.5)	36.0 (90.0)	
pRCC	2.0 (2.5)	1.0 (2.5)	1.0 (2.5)	
chRCC	3.0 (3.7)	2.0 (5.0)	1.0 (2.5)	
AML	2.0 (2.5)	0.0 (0.0)	2.0 (5.0)	
BMI, median (IQR), kg/m^2	24.2 (22.2, 27.0)	23.7 (21.5, 26.6)	24.4 (22.4, 27.2)	ns
HTN, No. (%)	30.0 (37.5)	18.0 (45.0)	12.0 (30.0)	ns
DM, No. (%)	23.0 (28.8)	8.0 (20.0)	15.0 (37.5)	ns
R.E.N.A.L score, No. (%)				ns
Low	16.0 (20.0)	7.0 (17.5)	9.0 (22.5)	
Intermediate	38.0 (47.5)	21.0 (52.5)	17.0 (42.5)	
High	26.0 (32.5)	12.0 (30.0)	14.0 (35.0)	
Duration of surgery, median (IQR), min	140.0 (120.0, 170.0)	128.0 (111.0, 156.0)	145.0 (125.0, 174.0)	0.037
Bleeding volume, median (IQR), ml	100.0 (50.0, 20.0)	50.0 (50.0, 10.0)	200.0 (100.0, 200.0)	< 0.001
Warm ischemia time, median (IQR), min	26.0 (22.0, 29.0)	24.0 (18.0, 27.0)	28.0 (25.0, 30.0)	< 0.001
No. of renal artery, No. (%)				ns
1	68.0 (85.0)	35.0 (87.5)	33.0 (82.5)	
>1	12.0 (15.0)	5.0 (12.5)	7.0 (17.5)	
Prehilar branching artery, No. (%)	20.0 (25.0)	9.0 (22.5)	11.0 (27.5)	ns
Artery anterior to the vein, No. (%)	34.0 (42.5)	18.0 (45.0)	16.0 (40.0)	ns
Vascular variations, No. (%)	48.0 (60.0)	23.0 (57.5)	25.0 (62.5)	ns
Complications, No. (%)				ns
Postoperative bleeding	1.0 (1.3)	1.0 (2.5)	1.0(2.5)	
Wound infection	2.0 (2.5)	1.0 (2.5)	1.0 (2.5)	
AKI	4.0 (5.0)	1.0 (2.5)	3.0 (7.5)	
Positive surgical margin	0.0 (0.0)	0.0 (0.0)	0.0 (0.0)	ns

Abbreviations: AKI, acute kidney injury; AML, angiomyolipoma; BMI, body mass index; ccRCC, clear cell renal cell carcinoma; chRCC, chromophobe cell carcinoma; DM, diabetes mellitus; HTN, hypertension; IQR, interquartile range; ns, no significance; pRCC, papillary renal cell carcinoma; R.E.N.A.L., the radius, exophytic, or endophytic properties, nearness of tumor to the collection system or sinus in millimeters, anterior or posterior location.

was 24.2 kg/m^2 (IQR: 22.2–27.0). Pertaining to comorbidities, hypertension (HTM) was present in 30 patients (37.5%), while diabetes mellitus (DM) affected 23 patients (28.8%). The R.E.N.A.L score, employed to assess tumor complexity, revealed that 16 patients (20.0%), 38 patients (47.5%), and 26 patients (32.5%) had low, intermediate, and high tumor complexity, respectively. No significant differences were observed in the R.E.N.A.L score between the two cohorts. The median duration of surgery was 140.0 min (IQR: 120.0–170.0). Interestingly, the 3D-Cohort exhibited a significantly shorter operation time (median: 128 min) compared with the 2D-Cohort (median: 145 min) ($P = 0.037$). Moreover, the 3D-Cohort experienced significantly less intraoperative bleeding volume than the 2D-Cohort (median: 50 ml vs 200 ml, $P < 0.001$). The application of warm ischemia was consistent across all patients, with a median ischemia time of 26 min. However, the 3D-Cohort demonstrated a significantly shorter intraoperative warm ischemia time compared with the 2D-Cohort (median: 24 min vs 28 min, $P < 0.001$). For vascular variations, we assessed the most common three kinds of variants, including the number of renal arteries, perihilar branching artery, and artery anterior to the vein. Of the total patient cohort, 48 patients (60%) exhibited at least one vascular variation, with 23 patients (57.5%) in the 3D-Cohort and 25 patients (62.5%) in the 2D-Cohort. The utilization of 3D reconstruction imaging allowed for a more comprehensive, intuitive, and accurate evaluation of vascular variations, as depicted in Fig. 1.

3.2. Difference in operative parameters between 3D-Cohort and 2D-Cohort

To ascertain whether preoperative assessment using 3D reconstruction enhances surgical outcomes, a comparison was made between the 3D-Cohort and 2D-Cohort in terms of operative data. The results revealed a significant superiority of the 3D-Cohort in terms of operation time ($P = 0.037$), intraoperative bleeding volume ($P < 0.001$), and warm ischemia time ($P < 0.001$) (Fig. 2A-C). Subsequently, the influence of vascular variations on surgical outcomes in different cohorts was examined. Interestingly, vascular variations had no significant effect on the duration of surgery ($P = 0.151$), bleeding volume ($P = 0.294$), or warm ischemia time ($P = 0.665$) in the 3D-Cohort (Fig. 2D-F). Conversely, in the 2D-Cohort, patients with vascular variations exhibited significantly longer operation time ($P < 0.001$), increased bleeding volume ($P = 0.010$), and prolonged warm ischemia time ($P = 0.014$). Furthermore, a comparison between surgical outcomes in patients with vascular variations in the 3D-Cohort and 2D-Cohort demonstrated that the 3D-Cohort still achieved a significantly shorter operation time ($P = 0.011$), reduced bleeding volume ($P = 0.009$), and shorter warm ischemia time ($P < 0.001$) (Fig. 2D-F). These results substantiate the efficacy of preoperative preparation based on the 3D reconstruction system in effectively reducing operation time, bleeding volume, and warm ischemia time for CERT, thereby improving surgical safety and patient prognosis.

3.3. Changes in relative eGFR after RAPN

Further investigation was conducted to determine the impact of vascular variation and warm ischemia time on postoperative eGFR in CERT. As depicted in Fig. 3A, the eGFR changes in the 2D-Cohort exhibited a significant decline compared with those in the 3D-Cohort. Similar findings were observed when comparing patients with warm ischemia time≥ 25 min (short-term eGFR changes: $P = 0.01$; long-term eGFR changes: $P = 0.02$, Fig. 3C). However, no significant differences in eGFR changes were observed between the 2D-Cohort and 3D-Cohort in patients with warm ischemia time less than 25 min (Fig. 3B). Notably, patients with vascular variations in the 2D-Cohort exhibited a significant decline in both short-term ($P = 0.01$) and long-term ($P = 0.04$) eGFR compared with patients without vascular variation (Fig. 3D). In contrast, no significant

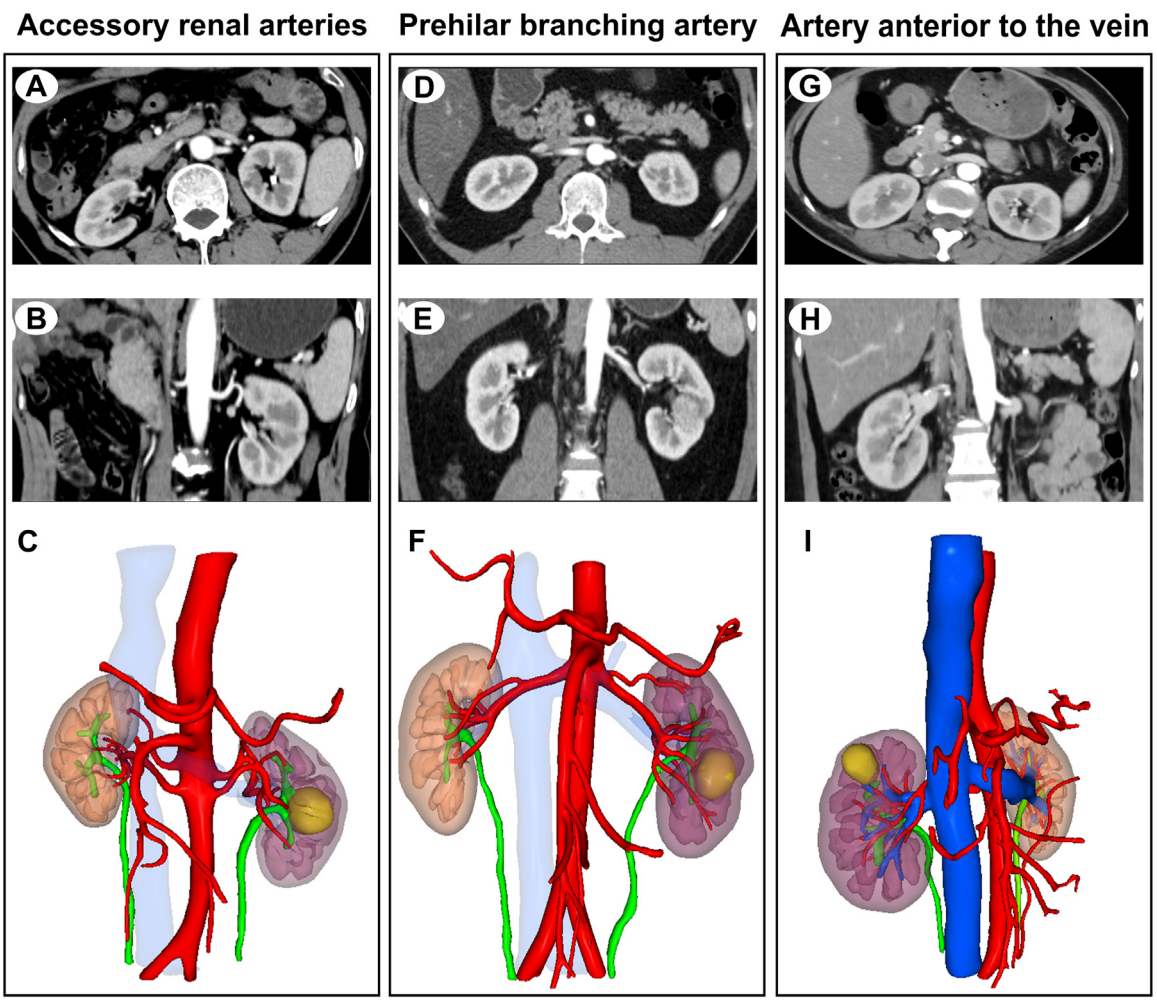

Fig. 1. Illustration of vascular variations. (A-I) Computed tomography and 3D reconstruction of variations of accessory renal arteries (A-C), prehilar branching artery (D-F), and artery anterior to the vein (G-I).

disparity in eGFR changes was observed in the 3D-Cohort (Fig. 3E), potentially attributable to the improved preoperative assessment of vascular factors facilitated by 3D reconstruction. This enhanced assessment may contribute to reduced warm ischemia time and increased preservation of nephrons. Furthermore, a comparative analysis was conducted to evaluate the extent of normal renal tissue margin surrounding the tumor capsule in the two cohorts. Notably, patients in the 2D-Cohort exhibited a larger margin of normal renal tissue (Fig. 4A-C), whereas patients in the 3D-Cohort demonstrated a smaller margin (Fig. 4D-F). The implementation of 3D reconstruction techniques proved beneficial in preserving more nephrons while concurrently enhancing surgical safety.

3.4. Construction and application of the RAL model

In summary, the utilization of a 3D reconstruction image in comparison with a traditional 2D image offers the advantage of enhanced assessment of vascular factors, resulting in reduced warm ischemia time, intraoperative blood loss, and renal function impairment. Consequently, this study aimed to optimize the R.E.N.A.L scoring system and develop an alternative model tailored to the specific demands based on 3D reconstructed images. The RAL model was constructed by incorporating parameters such as tumor size, vascular variations, and tumor location. The scoring system employed in this model assigned a score ranging from 1 to 3 for each component, which was subsequently summed to obtain the overall score, as depicted in Table 2.

The 40 patients in the 3D Cohort were categorized into low (8.7%), medium (31.2%), and high-risk (10%) groups based on their individualized RAL scores. The median age of the cohort was 56 years, comprising 24 males and 16 females. The findings demonstrated that higher RAL scores were associated with larger tumor sizes ($P = 0.006$), longer operative time ($P = 0.003$), and prolonged warm ischemia time ($P = 0.008$) within the patient cohort. Furthermore, a statistically significant correlation was observed between higher RAL scores and a more marked decrease in postoperative eGFR ($P = 0.019$). To evaluate the efficacy of the RAL model, we compared it with the R.E.N.A.L score, PADUA score, and CI score. The results revealed a significant correlation between higher RAL scores and higher R.E.N.A.L scores ($P = 0.003$) and CI scores ($P = 0.024$), as shown in Table 3. Moreover, the ROC curves demonstrated that the RAL scoring system (AUC = 0.857) exhibited superior predictive capabilities for postoperative eGFR changes compared with the R.E.N.A.L score (AUC = 0.649), PADUA score (AUC = 0.692), and CI score (AUC = 0.680) (Fig. 5).

4. Discussion

With a commonly higher R.E.N.A.L score, CERT represents a complex nephron-sparing procedure due to its intricate anatomical structure and invisibility, leading to significant postoperative renal function loss. Nevertheless, there are only a few studies that specifically report on CERT. The surgical management of CERT has undergone remarkable advance-

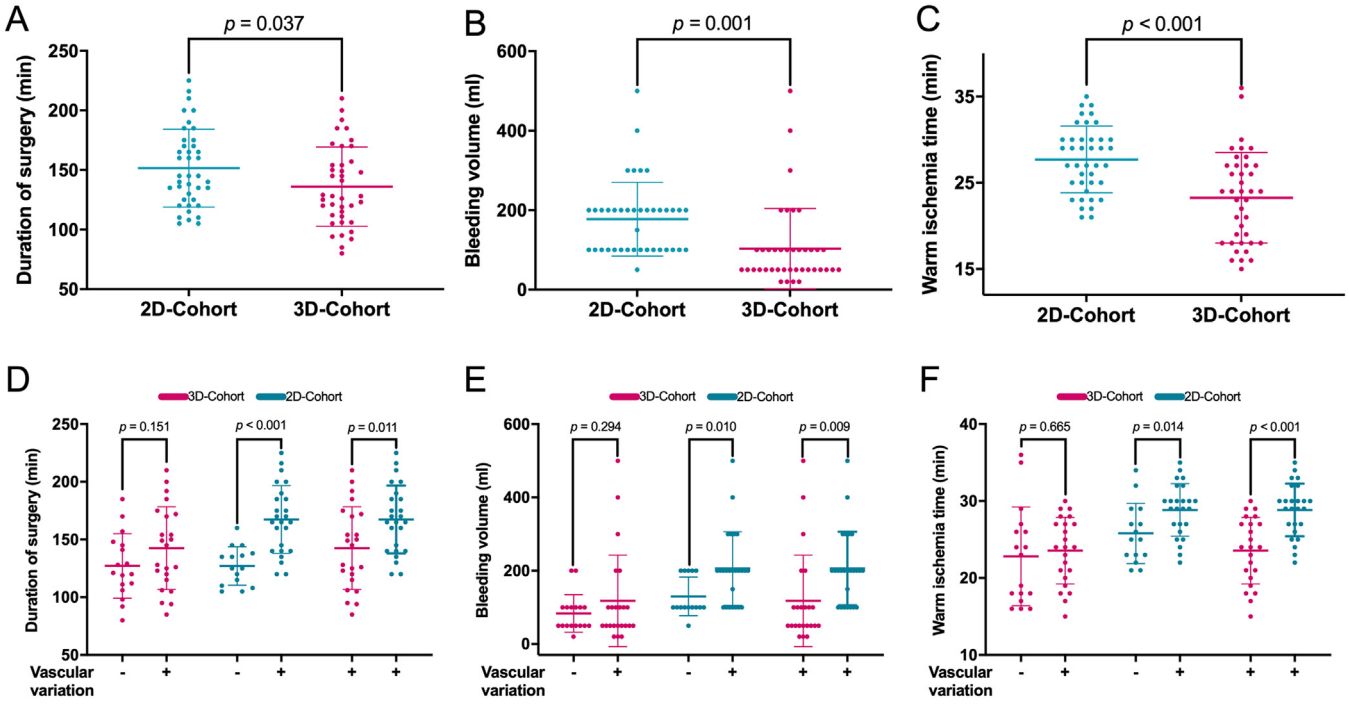

Fig. 2. Difference in operative parameters between 3D-Cohort and 2D-Cohort. (A-C) Comparison of surgery time (A), bleeding volume (B), and warm ischemia time (C) between 3D-Cohort and 2D-Cohort. (D-F) The impact of vascular variations on the operative parameters of surgery time (D), bleeding volume (E), and warm ischemia time (F) in 3D-Cohort and 2D-Cohort.

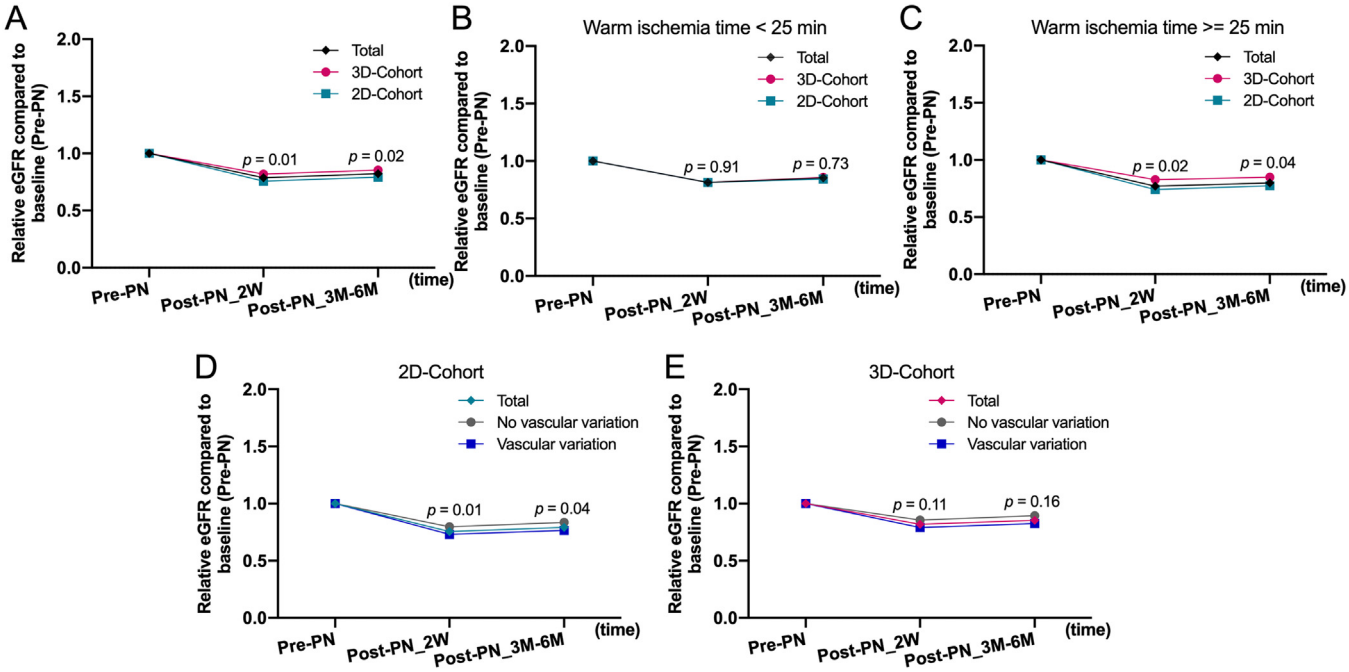

Fig. 3. Changes in relative eGFR after robot-assisted partial nephrectomy. (A-C) Changes in postoperative relative eGFR in 2D-and 3D-Cohort (A), Changes in relative eGFR in patients with warm ischemic time <25 min in both cohorts (B), and >= 25 min in both cohorts (C). (D and E) Effect of vascular variations on postoperative relative eGFR in 2D- (D) and 3D-Cohorts (E), respectively. eGFR, estimated glomerular filtration rate; M, month; PN, partial nephrectomy; W, week.

ments over the past few decades. Since the introduction of the da Vinci surgical system, RAPN, which was initially regarded as "still undergoing evaluation" by the European Association of Urology in 2010,[25] has been shown to produce similar or even superior outcomes compared with conventional LPN in systematic reviews and meta-analyses.[26,27] With its minimally invasive approach, RAPN excels in tumor detection and preserves a greater number of normal nephrons during CERT removal.[28] The use of cutting-edge technology has mitigated the high risk of intraoperative injury to the renal vessels and collecting system.

The majority of renal tumor scoring systems commonly rely on 2D imaging, which inherently limits their ability to comprehensively evaluate CERT. However, the advent of 3D imaging has provided a solution to this predicament by enabling improved precision in localizing CERT and enhancing agreement among observers. In this particular study, we en-

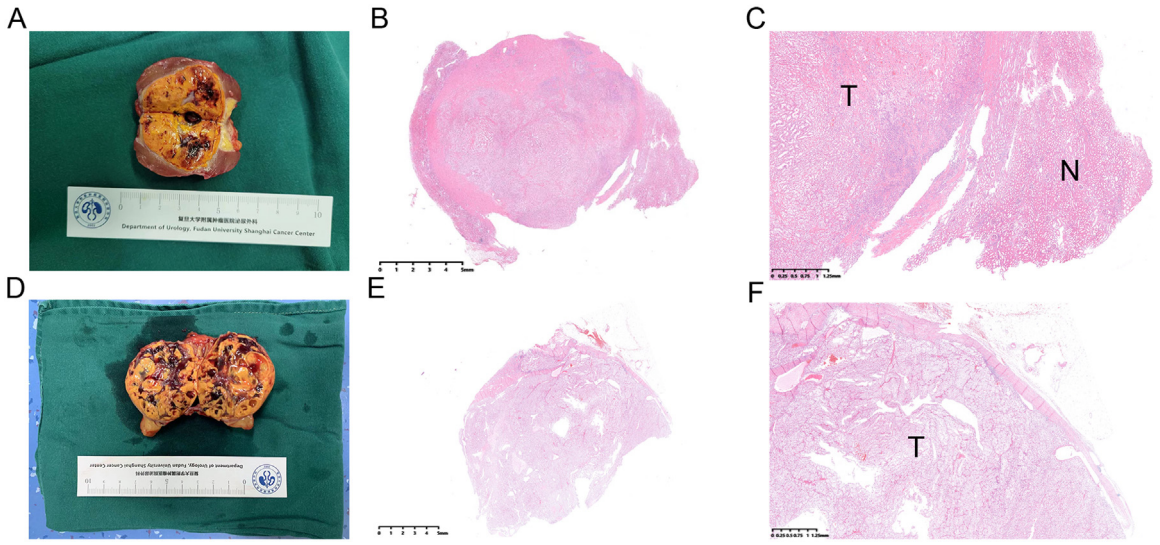

Fig. 4. Presentation of tumor margins in 2D and 3D-Cohort. (A) A representative image of patients assessed by 2D imaging reveals a greater extent of normal renal tissue surrounding the tumor capsule. (B and C) The histological examination (HE section) of the patient revealed an intact tumor capsule, with a notable presence of normal renal tissue surrounding it. (D) Representative images of patients assessed by 3D imaging show little normal renal tissue outside the tumor capsule. (E and F) The HE section of the patient indicated an intact tumor capsule, with no discernible presence of normal renal tissue outside the capsule. HE, hematoxylin-eosin staining.

Table 2
The RAL scoring system for assessing surgical complexity in completely endophytic renal tumors.

Component	RAL points		
	1	2	3
R: Radius (maximal diameter in cm)	$R \leq 2$	$2 < R \leq 4$	$R > 4$
A: Occurrence of arterial variations[a]	No	Only one vascular variation	Two or more vascular variations
L: Location relative to the polar lines	Entirely above the upper or below the lower polar line	Lesion crosses polar line	>50% of mass is across polar line or mass crosses the axial renal midline or mass is entirely between the polar lines

[a] Arterial variations include: more than one renal artery, prehilar branching artery and renal artery anterior to the renal vein. 1 point is given for no vascular variation, 2 points for 1 vascular variation, and 3 points for combining 2 or more vascular variations.

Table 3
Clinical and surgical characteristics, and other nephrometry scoring systems according to the RAL classification.

Variables	RAL classification				*P* value
	All	Low	Moderate	High	
3D-Cohort, No. (%)	40 (50)	7 (8.7)	25 (31.2)	8 (10.0)	
Age, median (IQR), years	56 (44, 66)	56 (49, 59)	56 (47, 66)	55 (34, 73)	ns
Gender, No. (%)					ns
Male	24 (60.0)	5 (71.4)	29 (72.5)	5 (62.5)	
Female	16 (40.0)	2 (28.6)	11 (27.5)	3 (37.5)	
Tumor size, median (IQR), cm	2.5 (1.8, 3.0)	1.5 (1.0, 2.0)	2.5 (2.0, 3.0)	2.8 (2.5, 3.8)	0.006
Duration of surgery, median (IQR), min	145 (116, 170)	120 (111, 148)	129 (109, 156)	182 (157, 192)	0.003
Bleeding volume, median (IQR), ml	50 (50, 100)	50 (50, 50)	100 (50, 100)	100 (75, 250)	ns
Warm ischemia time, median (IQR), min	22 (18, 27)	18 (16, 21)	22 (18, 27)	27 (24, 29)	0.008
Change in eGFR, median (IQR)[a]	14.1 (5.5, 21.1)	6.8 (−4.2, 11.5)	14.7 (3.9, 24.5)	20.0 (13.8, 42.9)	0.019
Nephrometry scoring system, median (IQR)					
R.E.N.A.L score	9 (8, 10)	7 (6, 8)	9 (8, 10)	10 (8, 11)	0.003
PADUA score	11 (10, 11)	10 (9, 11)	11 (10, 12)	11 (10, 12)	ns
CI score	1.5 (0.9, 1.9)	2.1 (1.6, 3.1)	1.6 (0.8, 1.9)	1.1 (0.7, 1.4)	0.024

Abbreviations: 3D, three-dimension; CI, centrality index; ns, no significance; eGFR, estimated glomerular filtration rate; IQR, interquartile range; PADUA: preoperative aspects and dimensions used for an anatomical classification; relative to polar lines nephrometry scoring system; RAL score, R indicates the maximal tumor radios; A, occurrence of arterial variations; L, location relative to the polar lines; R.E.N.A.L., the radius, exophytic, or endophytic properties, nearness of tumor to the collection system or sinus in millimeters, anterior or posterior location.

[a] Values indicate the changes from preoperative to 3–6 months postoperative levels.

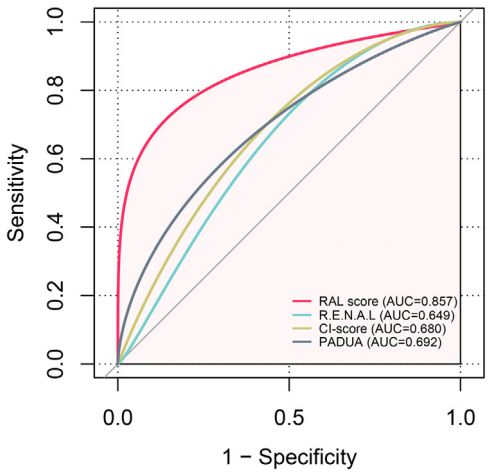

Fig. 5. Construction and application of the RAL model. Receiver operating characteristic curves of the RAL scoring system compared with traditional scoring systems (R.E.N.A.L, PADUA, and CI-score). AUC, area under the curve.

rolled a total of 80 patients with CERT, with 40 patients in each group, to compare intra- and postoperative variables in different dimensions between the 3D and 2D cohorts. Our findings indicate that 3D imaging offers a more accurate representation of the condition of CERT. Surgeries guided by 3D imaging demonstrated shorter durations, reduced hemorrhage volume, and decreased warm ischemia time. The favorable outcomes observed in the 3D cohort highlight the valuable role of 3D imaging in streamlining surgical procedures and preserving renal function. By leveraging precise anatomical insights, surgical decisions guided by 3D imaging optimize the management of complex tumors, with a primary focus on nephron preservation.[29]

Vascular variations have emerged as a critical factor influencing perioperative hemorrhage volume and ischemia time. Typically, each kidney is supplied by a single renal artery located behind the renal veins. However, our observations revealed a high prevalence of vascular variations in our cohorts, including accessory renal arteries, prehilar branching, and arteries located anterior to the veins. These variations present significant surgical challenges and increase the risk of bleeding. Importantly, the current preoperative evaluation for CERT does not encompass the assessment of vascular variations. Therefore, we aim to incorporate this factor into the development of a more precise and clinically relevant scoring system, termed the RAL scoring system. Our research demonstrates that the RAL scoring system exhibits greater sensitivity in evaluating CERT compared with the commonly used three scoring systems, as evidenced by the ROC curve. Furthermore, with the integration of 3D technology, images provide enhanced visualization of vascular distribution, leading to a reduction in the time spent in managing blood vessels and intraoperative hemorrhage volume.

The arterial-based complexity (ABC) scoring system, which also incorporates vascular elements involved, takes into consideration the relationship between renal tumor depth and the renal arterial vascular anatomy but fails to return a comprehensive view of the tumor as this system merely consists of vascular anatomic features.[30] The advent of 3D imaging technology has opened new horizons for visualizing renal lesions and achieving minimal invasiveness,[31-33] which has become the motivational factor of a revolutionary shift in the conventional systems. However, in recent years there have been not as many renal scoring systems based on 3D reconstruction of computerized tomography.[17,34] In contrast, our RAL scoring system distinguishes itself from existing systems by evaluating vascular variations, which, to our knowledge, have not ever been involved in the existing scoring systems. By achieving the combination of 3D imaging, vascular elements, and conventional indexes, it provides exhaustive predictive information, including surgery time, warm ischemia time, and nephron loss. Furthermore, it has an overarching role in the current systems, since a high RAL score usually suggests a high R.E.N.A.L, PADUA, and CI score, as shown in Table 3.

Conclusively, for the first time, we have formulated a RAL scoring system tailored for CERT, leveraging 3D reconstruction to appraise the impact of vascular considerations on intraoperative metrics and postoperative eGFR. Undertaking a PN for CERT presents a formidable technical challenge, even for seasoned surgeons. By means of preoperative 3D reconstruction from CT and a comprehensive assessment of surgical complexities, we endeavored to preserve maximal renal function in patients with the aid of robotic assistance and the RAL scoring system. The utilization of 3D reconstruction allows for a more precise localization of CERT, thereby mitigating superfluous loss of normal nephrons resulting from localization errors. Furthermore, RAPN minimizes nephron loss during suturing as compared with LPN. The ROC curve underscored the superiority of our system over conventional 2D-based systems in evaluating CERT. Nonetheless, due to constraints imposed by the cohort size, a validation of our RAL scoring system in a larger cohort is warranted. Consequently, the practicality of the RAL system necessitates corroborating evidence from multiple centers. Additionally, given the retrospective nature of this study, we aspire to prospectively assess the role of the RAL scoring system in the management of CERT.

Declaration of competing interest

The authors declare that they have no known competing financial interests or personal relationships that could have appeared to influence the work reported in this paper.

Ethics statement

All of the study designs and test procedures were performed in accordance with the Helsinki Declaration II. The Ethics approval and participation consent of this study was approved by the ethics committee of Fudan University Shanghai Cancer Center (approval number: 050432-4-1911D). All patients participating in this study signed informed consent forms.

Consent for publication

The patients whose medical images are presented in this manuscript provided consent for publication of their medical images for the manuscript. Only de-identified data and images are used in this article.

Acknowledgments

We thank researchers for patients enrolled from the FUSCC cohort. This work was supported by grants from the National Natural Science Foundation of China (grant numbers: 81802525 and no. 82172817), the Natural Science Foundation of Shanghai (grant number: 20ZR1413100), Beijing Xisike Clinical Oncology Research Foundation (grant number: Y-HR2020MS-0948), the Shanghai “Science and Technology Innovation Action Plan” medical innovation research Project (grant number: 22Y11905100), the Shanghai Anti-Cancer Association Eyas Project (grant number: SACA-CY21A06 and no. SACA-CY21B01), and Fudan University Fuqing scholars Project (grant number: FQXZ202304A).

Author contributions

W.H, Y.Z, H.L, and D.W designed the project; A.A, X.X, and L.S collected and analyzed the data; A.A, X.X, X.T, S.Q visualized the results; A.A and X.X wrote the original draft; W.H, Y.Z, H.L, and D.W contributed to writing, reviewing, and editing. The authorship order was agreed upon by all authors. All authors read and approved the final manuscript.

References

1. Siegel R, Miller K, Jemal A. Cancer statistics, 2019. *CA Cancer J Clin*. 2019;69(1):7–34.
2. Ljungberg B, Albiges L, Abu-Ghanem Y, et al. European association of urology guidelines on renal cell carcinoma: the 2022 update. *Eur Urol*. 2022;82(4):399–410.
3. Campbell S, Uzzo R, Allaf M, et al. Renal mass and localized renal cancer: AUA guideline. *J Urol*. 2017;198(3):520–529.
4. Larcher A, Capitanio U, De Naeyer G, et al. Is robot-assisted surgery contraindicated in the case of partial nephrectomy for complex tumours or relevant comorbidities? A comparative analysis of morbidity, renal function, and oncologic outcomes. *Eur Urol Oncol*. 2018;1(1):61–68.
5. Carbonara U, Simone G, Minervini A, et al. Outcomes of robot-assisted partial nephrectomy for completely endophytic renal tumors: a multicenter analysis. *Eur J Surg Oncol*. 2021;47(5):1179–1186.
6. Choi J, You J, Kim D, Rha K, Lee S. Comparison of perioperative outcomes between robotic and laparoscopic partial nephrectomy: a systematic review and meta-analysis. *Eur Urol*. 2015;67(5):891–901.
7. Leow J, Heah N, Chang S, Chong Y, Png K. Outcomes of robotic versus laparoscopic partial nephrectomy: an updated meta-analysis of 4,919 patients. *J Urol*. 2016;196(5):1371–1377.
8. Froghi S, Ahmed K, Khan M, Dasgupta P, Challacombe B. Evaluation of robotic and laparoscopic partial nephrectomy for small renal tumours (T1a). *BJU Int*. 2013;112(4):E322–E333.
9. Kutikov A, Uzzo RG. The R.E.N.A.L. nephrometry score: a comprehensive standardized system for quantitating renal tumor size, location and depth. *J Urol*. 2009;182(3):844–853.
10. Ficarra V, Novara G, Secco S, et al. Preoperative aspects and dimensions used for an anatomical (PADUA) classification of renal tumours in patients who are candidates for nephron-sparing surgery. *Eur Urol*. 2009;56(5):786–793.
11. Simmons MN, Ching CB, Samplaski MK, Park CH, Gill IS. Kidney tumor location measurement using the C index method. *J Urol*. 2010;183(5):1708–1713.
12. Kolla SB, Spiess PE, Sexton WJ. Interobserver reliability of the RENAL nephrometry scoring system. *Urology*. 2011;78(3):592–594.
13. Okhunov Z, Rais-Bahrami S, George AK, et al. The comparison of three renal tumor scoring systems: c-index, P.A.D.U.A., and R.E.N.A.L. nephrometry scores. *J Endourol*. 2011;25(12):1921–1924.
14. Benadiba S, Verin AL, Pignot G, et al. Are urologists and radiologists equally effective in determining the RENAL nephrometry score? *Ann Surg Oncol*. 2015;22(5):1618–1624.
15. Mashin GA, Kozlov VV, Chinenov DV, et al. Nephrometric score based on 3D modeling (3D nephrometry score) for the probability prediction of intra- and postoperative complications for kidney surgery. *Urologia*. 2022;89(2):179–184.
16. Yoshitomi KK, Komai Y, Yamamoto T, et al. Improving accuracy, reliability, and efficiency of the RENAL nephrometry score with 3D reconstructed virtual imaging. *Urology*. 2022;164:286–292.
17. Huang Q, Gu L, Zhu J, et al. A three-dimensional, anatomy-based nephrometry score to guide nephron-sparing surgery for renal sinus tumors. *Cancer*. 2020;126(Suppl 9):2062–2072.
18. Famurewa OC, Asaleye CM, Ibitoye BO, Ayoola OO, Aderibigbe AS, Badmus TA. Variations of renal vascular anatomy in a Nigerian population: a computerized tomography studys. *Niger J Clin Pract*. 2018;21(7):840–846.
19. Çınar C, Türkvatan A. Prevalence of renal vascular variations: evaluation with MDCT angiography. *Diagn Interv Imaging*. 2016;97(9):891–897.
20. Aristotle S, Sundarapandian, Felicia C. Anatomical study of variations in the blood supply of kidneys. *J Clin Diagn Res*. 2013;7(8):1555–1557.
21. Thompson RH, Lane BR, Lohse CM, et al. Every minute counts when the renal hilum is clamped during partial nephrectomy. *Eur Urol*. 2010;58(3):340–345.
22. Simmons MN, Hillyer SP, Lee BH, Fergany AF, Kaouk J, Campbell SC. Functional recovery after partial nephrectomy: effects of volume loss and ischemic injury. *J Urol*. 2012;187(5):1667–1673.
23. Khalifeh A, Autorino R, Hillyer SP, et al. Comparative outcomes and assessment of trifecta in 500 robotic and laparoscopic partial nephrectomy cases: a single surgeon experience. *J Urol*. 2013;189(4):1236–1242.
24. Levey AS, Bosch JP, Lewis JB, Greene T, Rogers N, Roth D. A more accurate method to estimate glomerular filtration rate from serum creatinine: a new prediction equation. Modification of Diet in Renal Disease Study Group. *Ann Intern Med*. 1999;130(6):461–470.
25. Ljungberg B, Cowan NC, Hanbury DC, et al. EAU guidelines on renal cell carcinoma: the 2010 update. *Eur Urol*. 2010;58(3):398–406.
26. Aboumarzouk OM, Stein RJ, Eyraud R, et al. Robotic versus laparoscopic partial nephrectomy: a systematic review and meta-analysis. *Eur Urol*. 2012;62(6):1023–1033.
27. Froghi S, Ahmed K, Khan MS, Dasgupta P, Challacombe B. Evaluation of robotic and laparoscopic partial nephrectomy for small renal tumours (T1a). *BJU Int*. 2013;112(4):E322–E333.
28. Carbonara U, Simone G, Minervini A, et al. Outcomes of robot-assisted partial nephrectomy for completely endophytic renal tumors: a multicenter analysis. *Eur J Surg Oncol*. 2021;47(5):1179–1186.
29. Amparore D, Piramide F, Pecoraro A, et al. Identification of recurrent anatomical clusters using three-dimensional virtual models for complex renal tumors with an imperative indication for nephron-sparing surgery: new technological tools for driving decision-making. *Eur Urol Open Sci*. 2022;38:60–66.
30. Spaliviero M, Poon BY, Karlo CA, et al. An Arterial Based Complexity (ABC) scoring system to assess the morbidity profile of partial nephrectomy. *Eur Urol*. 2016;69(1):72–79.
31. Piramide F, Kowalewski KF, Cacciamani G, et al. Three-dimensional model-assisted minimally invasive partial nephrectomy: a systematic review with meta-analysis of comparative studies. *Eur Urol Oncol*. 2022;5(6):640–650.
32. Amparore D, Pecoraro A, Checcucci E, et al. Three-dimensional virtual models' assistance during minimally invasive partial nephrectomy minimizes the impairment of kidney function. *Eur Urol Oncol*. 2022;5(1):104–108.
33. Porpiglia F, Checcucci E, Amparore D, et al. Three-dimensional augmented reality robot-assisted partial nephrectomy in case of complex tumours (PADUA ≥10): a new intraoperative tool overcoming the ultrasound guidance. *Eur Urol*. 2020;78(2):229–238.
34. Liu J, Liu J, Wang S, et al. Three-dimensional nephrometry scoring system: a precise scoring system to evaluate complexity of renal tumors suitable for partial nephrectomy. *PeerJ*. 2020;8:e8637.